

Mark Libardoni¹
Ernest Hasselbrink²
J. Hunter Waite³
Richard Sacks¹

Original Paper

At-column heating and a resistively heated, liquid-cooled thermal modulator for a low-resource bench-top GC × GC

¹Department of Chemistry,
University of Michigan, Ann
Arbor, MI, USA

²Department of Mechanical
Engineering, University of
Michigan, Ann Arbor, MI, USA

³Department of Atmospheric,
Oceanic and Space Science,
University of Michigan, Ann
Arbor, MI, USA

A transportable GC × GC instrument is under development for on-site applications that would benefit from the enhanced resolution and powers of detection, which can be achieved by this method. In the present study, a low-resource GC × GC instrument using an electrically heated and liquid-cooled single-stage thermal modulator that requires no cryogenic materials is evaluated. The instrument also uses at-column heating, thus eliminating the need for a convection oven to house the two columns. The stainless-steel modulator tube is coated with PDMS, which can be heated to 350°C for sample injection into the second-dimension column. The modulator is cooled to -30°C by a 100 mL/min flow of PEG by means of a commercial liquid chiller and a small recirculating pump. Resistive heating of the modulator tube is provided by a programmable power supply, which uses a voltage program that results in increasing modulator temperature during an analysis. This, together with more rapid cooling by the use of a liquid cooling medium, results in reduced solute breakthrough following each heating cycle as the modulator cools to a temperature where quantitative trapping resumes. As a result, modulated peak widths at half height of less than 40 ms are observed. Design and performance details are presented along with chromatograms of gasoline and an essential oil sample.

Keywords: GC × GC / Instrument design and development / Modulator

Received: July 28, 2005; revised: February 8, 2006; accepted: February 9, 2006

DOI 10.1002/jssc.200500298

1 Introduction

Comprehensive 2-D GC (GC × GC) has become an important method for the analysis of mixtures containing volatile and semivolatile organic components [1–5]. The large peak capacity, structured chromatograms, and increased level of detectability are favorable attributes that allow GC × GC to be used for qualitative and quantitative analyses of petroleum samples [6, 7], pesticides and other environmentally significant samples [8, 9], essential oils [10, 11], large-volume air samples for trace level components [12], and even human breath analysis (Libardoni, M., Waite, J. H., Sacks, R., *J. Chromatogr. B* 2006, submitted).

A typical GC × GC instrument consists of two capillary columns interfaced by means of a concentration modulation device. The first-dimension column is traditionally

nonpolar and can range from 10 to more than 60 m in length. The second-dimension column is traditionally polar and significantly shorter in length and smaller in diameter. This reduction in length and internal diameter provides a fast secondary separation of compounds that are released from the modulation device [13].

Various modulation devices have been described for GC × GC. Commercially available thermal modulators use cryogenic gases to trap the effluent released from the primary column [14, 15]. A few seconds later a jet of hot gas or heat from the GC oven is used to release the focused aliquot for a rapid second-column analysis. Most commercial modulation devices use the first few centimeters of the second-dimension column for modulation [16, 17].

The need for large amounts of cryogenic gases to efficiently trap components in the modulator is one disadvantage of commercially available GC × GC systems [18]. This need for consumables limits this technology to laboratory-based instruments. Eliminating cryogenic consumables and decreasing the weight and size of the

Correspondence: Dr. Mark Libardoni, 815 Pilot Rd. Suite C, Las Vegas, NV 89119, USA.

E-mail: mark_libardoni@leco.com.

Fax: +1-702-614-1189.

Abbreviation: FID, flame ionization detector

GC would allow this technology to become field deployable for on-site analysis.

To this end, an air-cooled, resistively heated single-stage thermal modulator has been described recently [19]. The device uses a commercially available stationary-phase coated metal capillary tube as the modulator. The modulator tube is cooled to about -30°C by a 35-L/min flow of cold air obtained from a conventional two-stage compressor-based refrigeration unit coupled to a heat exchanger. Every few seconds, the modulator tube is resistively heated by a current pulse from a power supply. The system uses only electrical power, carrier, and detector gas, and is transportable. However, the ability to transport a relatively large and heavy refrigeration unit is a major limitation for field portability and on-site analysis.

The use of liquid as a medium for cooling the modulator has an advantage over air cooling because the thermal conductivity of liquid is more favorable than air. In addition, with an effective heat exchanger and miniaturized recirculating pump, the size of the overall cooling system can be reduced substantially relative to the size of the previously described air-cooled system. Further, elimination of the conventional GC as a platform can result in a large reduction of instrument size and weight. This can be accomplished by using at-column heating for the two columns [20, 21]. This report describes the design and performance evaluation of a transportable GC \times GC that uses no convection oven and requires no consumables other than electric power, carrier gas, and gas for the flame ionization detector (FID). The thermal modulator is based on the previously described single-stage device [19] except liquid rather than air cooling is used. In addition, a programmable power supply is used for modulator heating that allows for on-the-fly changes in the modulator heating profile during an analysis.

2 Experimental

2.1 Apparatus

Figure 1a shows the design of the experimental system, and Fig. 1b shows details of the single-stage, liquid-cooled thermal modulator. The GC \times GC system is built on a 36 inch by 32 inch optical breadboard. A stand-alone HP 6890 split/splitless injector mounted on the breadboard is coupled to a 30-m long \times 0.25-mm id \times 0.25- μm film thickness PDMS (RTX-1, Restek, Bellefonte, PA) fused-silica first-dimension column. The downstream end of the first-dimension column is connected to an 8-cm long \times 0.18-mm id \times 0.20- μm film thickness PDMS (MXT-1, Restek) stainless-steel thermal modulator tube. The downstream end of the modulator is connected to a 2.0-m long \times 0.10-mm id \times 0.10- μm film thickness PEG (RTX-Wax, Restek) fused-silica column. A stand-alone FID (Var-

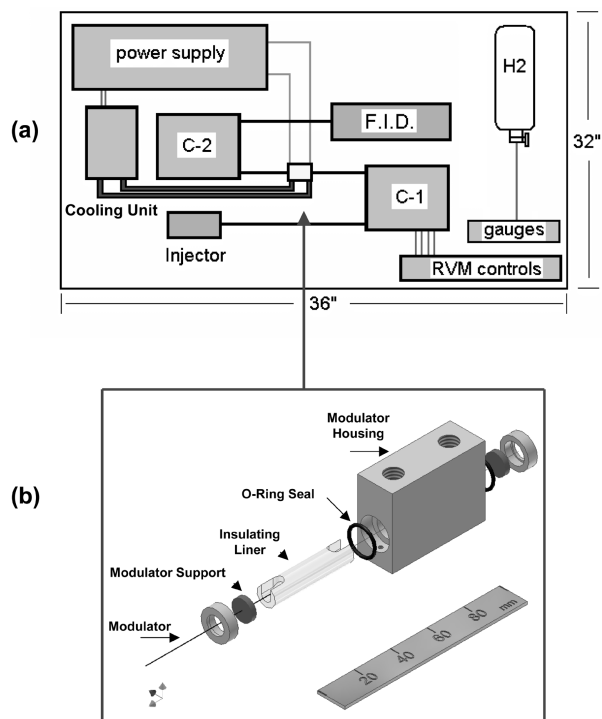


Figure 1. Instrument schematic and layout for the benchtop GC \times GC (a). Inset (b) displays the single-stage resistively heated thermal modulator. Electrical contacts from the power supply are made directly to the modulator tube immediately adjacent to the modulator supports. Modulator drawing courtesy of Bruce Block, University of Michigan Space Physics Research Laboratory.

ian, Palo Alto, CA) is used at the downstream end of the system with a high-speed (5 ms time constant) electrometer (Chromatofast, Ann Arbor, MI).

Machined aluminum blocks are used to house the injector and transfer lines. These parts are independently heated and controlled with variable temperature controllers (Omega 6100, Omega Engineering, Stamford, CT) thereby eliminating any cold spots. Thermocouples were attached to the machined blocks, with high-temperature adhesive strips, and routed to the Omega controllers.

The independently heated fused-silica columns use at-column heating, where the colinear ensemble of the column, heating wire, and temperature sensor are wrapped with fiber insulation, wound into a 4-inch coil, and covered with a sheath of aluminum foil. Electrical leads for the heating elements and the temperature sensor exit the insulation and attach to the power supply and electronic controls. Both columns were prepared at RVM Scientific, Santa Barbara, CA. Electronic controls for column heating were also provided by RVM Scientific.

The liquid-cooled thermal modulator has been previously discussed and evaluated for air-cooling [19].

Briefly, a Kevlar wrapped machined aluminum block houses the 8.0-cm-long piece of MXT-1 tubing that is coated with a thin film of PDMS. The modulator tube is centered through the block by means of standard 11.0 mm septa. A machined ceramic insulating liner located inside the modulator housing is used to prevent electrical contact between the modulator tube and housing. Electrical contacts are made outside the modulator housing directly on the modulator tube. A closed-loop recirculating laboratory chiller (Thermo Neslab RTE 420, Thermo Electron) is used to continually circulate ethylene glycol through the modulator housing at a temperature of -30°C and a flow rate of 100 mL/min. A programmable power supply (Agilent 6673A, Agilent, Palo Alto, CA) is used to provide an electrical current through the modulator tube for rapid heating.

2.2 Materials and procedures

Resistive heating of the modulator tube is carried out by a waveform file sent to the Agilent power supply *via* a computer and an analog/digital board. Previous studies used a fixed voltage applied to the modulator tube [19]. For this study, a programmable power supply was used, and voltage could be changed during an analysis. Studies were conducted to determine the power supply voltage, as a function of solute boiling point, required to minimize injection plug widths into the second column and reduce sample loss through the modulator during the cooling interval following each modulator heating pulse. Three replicate runs were performed on single compounds at each voltage. Peak width at half-height and integrated area of the modulated peaks were determined for each voltage. In all cases, the modulation period was 5.0 s.

Data from the FID are logged at a sampling rate of 100 Hz by means of a 16-bit A/D board (PC1-DAS1602/16, Measurement Computing, Middleboro, MA) and a PC. Data are initially stored as a 1-D text file, and then processed into a matrix based on the modulation period using MatLab software (The Math Works, Natick, MA). Peak areas and widths were measured from individual modulated peaks by Grams Spectral Notebook software (Thermo Galactic, Salem, NH).

Quantitative evaluation of the modulator was carried out by injections of a mixture of normal alkanes ranging from C_5 to C_{17} along with selected polar compounds. Calibration plots (integrated peak area *vs.* concentration) were obtained, and dynamic range and RSD values ($N = 3$) were calculated over three orders of magnitude concentration. LODs for the alkane series and polar compounds were determined by extrapolation of the plotted data to three times the S/N .

Chromatograms were obtained from a weathered gasoline sample and a lemon thyme essential oil sample. For

all experiments, the inlet, detector and all transfer lines were heated to 250°C in order to eliminate cold spots. In all cases, the inlet pressure was 55 psi \cdot g. Hydrogen was used as carrier gas after passage through filters for oxygen, water vapor, and hydrocarbons. Characterization of the essential oil was carried out on a commercially available LECO Pegasus 4D GC \times GC-TOFMS instrument (LECO, St. Joseph, MI) and compared with the data obtained from the bench-top GC \times GC-FID instrument described here. Similar column dimensions, stationary phases of the two columns, and temperature programming were used on both instruments. The TOF mass spectrometer was operated at a scan rate of 100 spectra/s over a mass range from 30 to 350 Da.

3 Results and discussion

3.1 Liquid cooling

Straightforward dimensional analysis common in most heat transfer texts shows that for a fixed geometry, forced-convection heat transfer with single-phase flow can be characterized by a simple functional dependence of the Nusselt number (Nu) as shown in Eq. (1) [22, 23].

$$Nu = [hD/k_f] \quad (1)$$

The Nusselt number is an important dimensionless parameter that represents the temperature gradient at a surface where heat transfer by convection is taking place. Here, h is the heat transfer coefficient, D is the outer diameter of the modulator, and k_f is the thermal conductivity of the cooling fluid. The Nusselt number can also be expressed as a function of the Reynolds number (Re) and the Prandtl number (Pr) as shown in Eq. (2).

$$Nu = f(Re, Pr) \quad (2)$$

The Reynolds number is important in analyzing any type of flow when there is a substantial velocity gradient or shear. The Reynolds number indicates the relative significance of viscous effects compared to inertia effects of the fluid flow. The Reynolds number is proportional to inertial force divided by viscous force, and can be expressed as shown in Eq. (3).

$$Re = [DV\rho/\mu] \quad (3)$$

Here ρ is the fluid density, V is the fluid flow speed over the modulator, and μ is the dynamic viscosity of the fluid.

The Prandtl number as shown in Eq. (2) is a dimensionless parameter of a convection system that characterizes the behavior of convection. It can be expressed as Eq. (4):

$$Pr = k_f/c_p\mu \quad (4)$$

Here c_p is the specific heat of the fluid.

When Nu is small (<1), it implies that the flow is so slow that direct thermal conduction in the fluid is more important than any additional cooling from the fluid motion. When Nu is larger than 1, convective cooling becomes increasingly more dominant. For flow over cylinders, a large volume of data exists from numerous sources showing expressions for various cylinder sizes in different fluids flowing at different speeds. Churchill and Bernstein [24] give a useful correlation as shown in Eq. (5):

$$Nu = 0.3 + \frac{0.62 Re^{1/2} Pr^{1/3}}{[1 + (0.4/Pr)^{2/3}]^{1/4}} \left[1 + \left(\frac{Re}{282000} \right)^{5/8} \right]^{4/5} \quad (5)$$

While this correlation appears complex, it simply expresses the fact that heat transfer from a cylinder increases monotonically with the speed of the flow around it. Two things are patently clear from this correlation. First, the correlation shows that at modest Reynolds numbers (laminar flow) the heat transfer scales only with the square root of the flow speed across it. Second, at a fixed Pr and Re , the use of low-thermal-conductivity cooling fluid (*e.g.*, gases) results in a fairly low heat transfer coefficient.

Therefore, if rapid cooling is desired, the only ways to make dramatic improvements in this regard (for a fixed geometry) are to increase the flow speed, thus increasing Re , or dramatically increase k_f . For the case of increasing Re with a cooling gas, previous studies showed that with the available heat exchanger and cooling device a minimum temperature of -32°C was achieved with a recirculating air flow rate of 35 L/min. In order to double the heat transfer, the gas flow rate would have to be increased to 140 L/min. This is impractical for the present system. For liquid cooling, k_f is orders of magnitude larger than for gas cooling, and thus rapid cooling can be achieved with relatively low-fluid flow velocity. Note that the modulator housing used in the present study also was used previously with air cooling. The flow velocity of the ethylene glycol cooling liquid is 350-fold lower than the air flow.

3.2 Modulator performance

The modulator used in this study is coated with a nonpolar film of PDMS, which can be heated to 350°C with minimal decomposition. This relatively high upper temperature limit is useful for the reinjection as narrow plugs of higher boiling point compounds into the second-dimension column. However, such high reinjection temperatures are unnecessary in order to obtain narrow reinjection plugs for more volatile compounds. In addition, a lower modulator temperature during a heating pulse may result in the more rapid return of the modula-

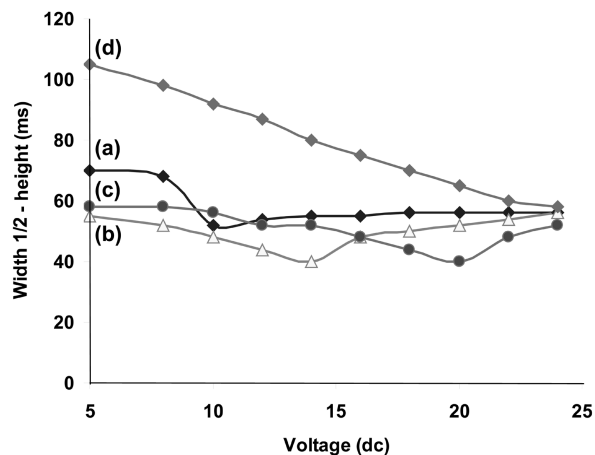


Figure 2. Peak width at half-height as a function of applied voltage for selected alkanes; (a) *n*-pentane, (b) *n*-heptane, (c) *n*-decane, and (d) *n*-dodecane. Minimum peak width at half-height achieved corresponds to the optimal voltage needed for reinjection into the second dimension.

tor temperature to a value where quantitative trapping (no breakthrough) occurs.

In order to reduce the amount of sample loss by breakthrough while the modulator is cooling from a heating cycle, an adjustable voltage was applied to control the modulator temperature. Tailoring the temperature of the modulator with respect to compound volatility can reduce sample loss for volatile compounds while preserving narrow injection plugs for the higher boiling compounds.

Figure 2 displays data collected for selected alkanes using different voltages applied to the modulator. Data are based on triplicate runs performed under the same operating conditions. A $1 \mu\text{L}$ injection of a $5000 \text{ pg}/\mu\text{L}$ solution with a split flow of 100:1 was used for each compound. Peak width at half-height is plotted *versus* the applied voltage for *n*-pentane (a), *n*-heptane (b), *n*-decane (c), and *n*-dodecane (d). The alkanes show minimal retention on the second, polar column and give a good representation of the modulated peak widths. The upper voltage limit was 24 V, since at higher voltages, a baseline shift was observed suggesting stationary-phase bleed from the modulator.

For pentane, a minimum peak width at half-height of 53 ms is observed for an applied voltage of 10 V. A slight increase in peak width at half-height is observed for higher voltages. For heptane, the minimum peak width at half-height is 40 ms and this occurs with an applied voltage of 14 V. Either an increase or a decrease in voltage results in an increase in peak width at half-height with values of 60 ms observed at 5 V and at 24 V. For decane, the minimum peak width at half-height again is 40 ms but the voltage required to obtain this minimum

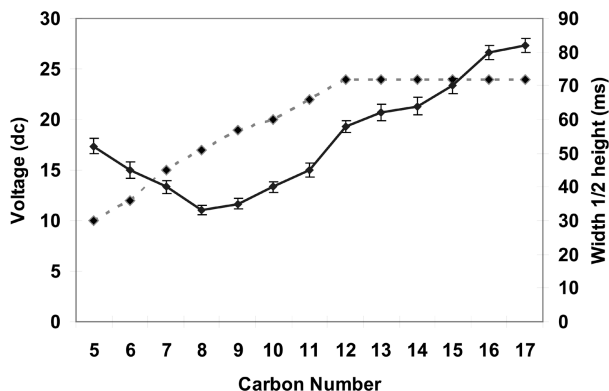


Figure 3. Graph of optimal voltage (dotted line) and modulated peak width at half-height (solid line) as a function of carbon number. Increasing the voltage to the modulator during the analysis optimizes the modulated peak widths for increased performance.

peak width at half-height has shifted to 20 V. For dodecane, the peak width at half-height decreases steadily with increasing applied voltage from 105 ms at 5 V to 58 ms at 24 V.

Based on the data from Fig. 2, the voltage program (applied voltage vs. carbon number) shown by the dashed line in Fig. 3 was used for all further studies. Figure 3 also displays the full width at half-height for the alkanes (solid line) using the indicated modulator heating program. Error bars show the SD of the measured peak width at half-height for three replicate experiments covering a boiling point range from n -C₅ to n -C₁₇. A minimum peak width at half-height of 33 ms was observed for n -C₈. The peak width increases to about 82 ms for n -C₁₇.

The data for liquid cooling are in qualitative agreement with previously reported data using the same modulator but with air cooling [19]. For alkanes more volatile than n -C₈, migration in the modulator tube during the trapping interval (5 s) results in increased plug length in the modulator prior to heating and thus results in increasing peak width with increasing volatility. For compounds less volatile than n -C₈, an increase in peak width is observed with decreasing compound volatility due to increased retention in the modulator during a heating pulse [19].

Figure 4 shows the GC × GC chromatogram for an n -C₅ to n -C₁₇ alkane mixture. The temperature programming rate was 30°C isothermal for 3 min followed by a 5°C/min ramping ending at 200°C for the first column. The second column began with a +30°C offset and followed the same ramping rate ending at 230°C. A modulation period of 5.0 s was used for the alkane analysis. The heating voltage program shown in Fig. 3 was used. The inset within the GC × GC chromatogram shows the 1-D modu-

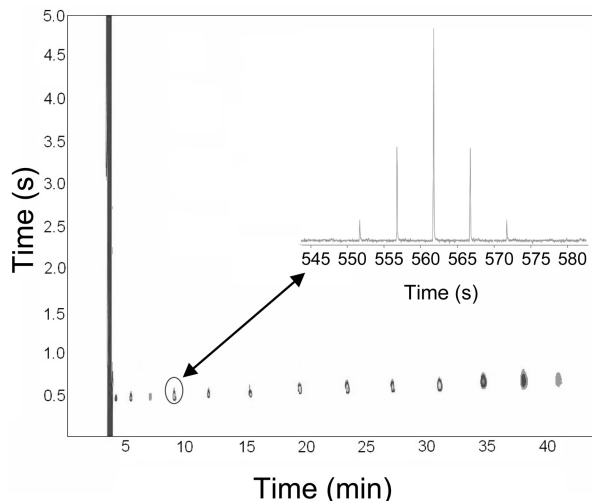


Figure 4. GC × GC chromatogram of n -C₅ through n -C₁₇ using the optimal voltage profile as described in Fig. 3. Inset is an expanded 1-D view of n -C₈ modulation. Depending on concentration, the modulated peak widths at half-height can be as narrow as 30 ms. Temperature programming rate was 30°C isothermal for 3 min followed by a 5°C/min ramping ending at 200°C for the primary column. Second column began with a +30°C offset and followed the same ramping rate ending at 230°C. A modulation period of 5.0 s was used.

lated n -C₈ peak with five modulations in which the compound is detected. There are no apparent artifacts, and peak tailing is minimal in both dimensions.

Quantitative experiments were carried out using the n -C₅ through n -C₁₇ alkane mixture along with selected polar compounds. Serial dilutions were made from a stock solution, and replicate runs ($n = 3$) were performed over a range of 2–5000 pg. Initial temperature of the first column was 30°C. The second column began with a +30°C offset. Both columns were held for 3 min under isothermal conditions followed by a 5°C/min temperature ramp to 220 and 250°C for the two columns, respectively.

Table 1 gives statistical data for the calibration plots. The log integrated area versus log sample mass trend lines are fitted for a range of 2–1000 pg. Log–log slopes are also presented from previously reported data [19] for the same modulator but using air cooling. Log versus log slopes signify the amount of sample transfer through the system, with the greatest amount of sample loss occurring within the modulation process. A reported slope of 1.00 signifies 100% sample transfer just as a reported slope of 0.92 would represent 92% sample transfer, or an 8% loss of sample. As sample mass begins to exceed about 1 ng, severe nonlinearity is observed for all the compounds, and integrated peak areas become nearly independent of sample concentration. This suggests that sample loss is large at higher concentrations as the modulator becomes overloaded.

Table 1. Quantitative data for polar and nonpolar compounds. Log–log slopes are for a previously reported modulator using air-cooling [19] and the liquid-cooled modulator used in this study. As the slopes approach 1.0, sample loss through the system is reduced. See text for complete details

| No. | Compound | Log vs. log slope ^{a)} | |
|-----|--------------|---------------------------------|---------------------|
| | | Single-stage air | Single-stage liquid |
| 1 | Pentane | 0.85 | 0.92 |
| 2 | Hexane | 0.88 | 0.96 |
| 3 | Heptane | 0.90 | 0.98 |
| 4 | Octane | 0.91 | 0.98 |
| 5 | Nonane | 0.92 | 0.97 |
| 6 | Decane | 0.92 | 0.96 |
| 7 | Undecane | 0.93 | 0.98 |
| 8 | Dodecane | 0.92 | 0.98 |
| 9 | Tridecane | 0.92 | 0.98 |
| 10 | Tetradecane | 0.92 | 0.96 |
| 11 | Pentadecane | 0.91 | 0.97 |
| 12 | Hexadecane | 0.92 | 0.97 |
| 13 | Heptadecane | 0.92 | 0.97 |
| 14 | Benzene | 0.92 | 0.97 |
| 15 | Toluene | 0.92 | 0.96 |
| 16 | 2-Pentanone | 0.92 | 0.97 |
| 17 | Benzaldehyde | 0.92 | 0.96 |
| 18 | m-Xylene | 0.93 | 0.96 |
| 19 | 2-Heptanone | 0.94 | 0.97 |
| 20 | 1-Pentanol | 0.94 | 0.97 |

^{a)} Mass range from 2 to 1000 pg.

For sample mass in the range 2–1000 pg, the early eluting compounds *n*-pentane and *n*-hexane give log–log trend line slopes of 0.92 and 0.96, respectively. This suggests that sample loss was occurring; however, it was reduced relative to the data previously reported with the air-cooled system. This is true for all compounds evaluated. As the volatility of the compounds decreases, the slopes of the plots approach 1.000 with a slope of 0.99 for decane and 2-heptanone. Reported RSDs ($N = 3$) are all below 1.5% with the higher boiling components having RSDs below 1.0%. Extrapolation of the plotted data to three times the S/N gave LOD for the liquid-cooled modulator in the low femtogram range, values lower than previously reported with air cooling. This observed performance increase is primarily due to the lower noise level associated with the electrometer used with the Varian FID as apposed to the system used in previous studies [19].

3.3 Sample chromatograms

Chromatogram quality was compared using a fixed voltage of 24 V and the programmable voltage waveform shown in Fig. 3. Figure 5 shows two chromatograms of a gasoline sample. A 1.0- μ L injection was used with a split ratio of 100:1. Column temperatures were set a 30 and 50°C for the first and second column, respectively. After

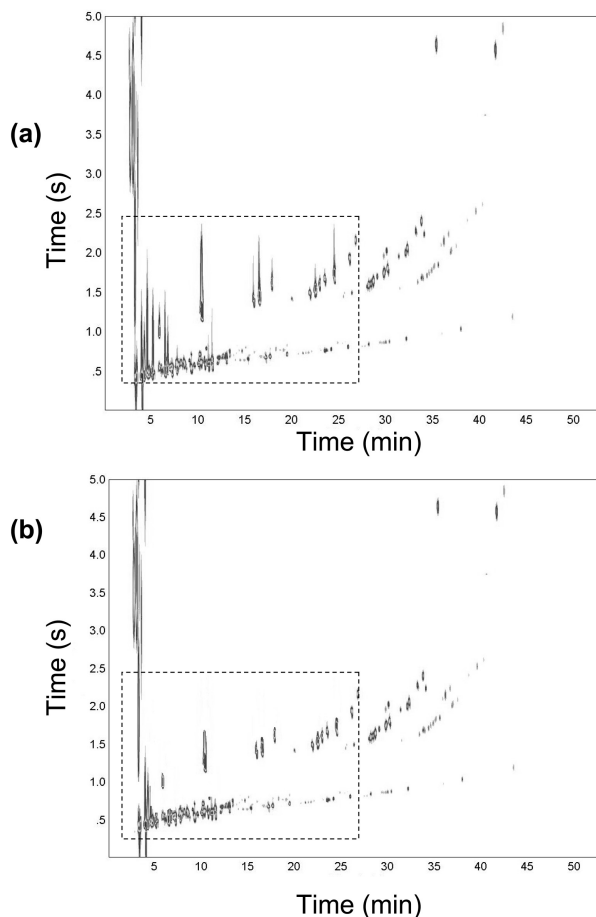


Figure 5. Chromatograms of a gasoline sample analyzed with the low-resource breadboard GC \times GC system. Inset (a) was performed with a constant modulator voltage of 25 V (dc). Inset (b) was performed with a variable voltage as described in Fig. 3. Dashed box shows a region of compound volatility where a decrease in peak streaking is observed when a variable voltage to the modulator is used. A 1.0- μ L injection was used with a split ratio of 100:1. Column temperatures were set a 30 and 50°C for the first and second column, respectively. After a 3 min isothermal period, each column was ramped at 5°C/min until the columns reached 200 and 220°C.

a 3 min isothermal period, each column was ramped at 5°C/min until the columns reached 200 and 220°C, respectively. A modulation period of 5 s was used.

Figure 5a was obtained with the fixed voltage, and Fig. 5b was obtained with the programmed voltage. The dashed box in each chromatogram highlights the area of high-volatility compounds relative to the boiling point range of the sample. When a constant voltage, which is high enough to obtain narrow reinjection plugs for the higher boiling point components, is used, peak streaking occurs along the second-dimension time axis, especially for highly volatile compounds. This is a result of the modula-

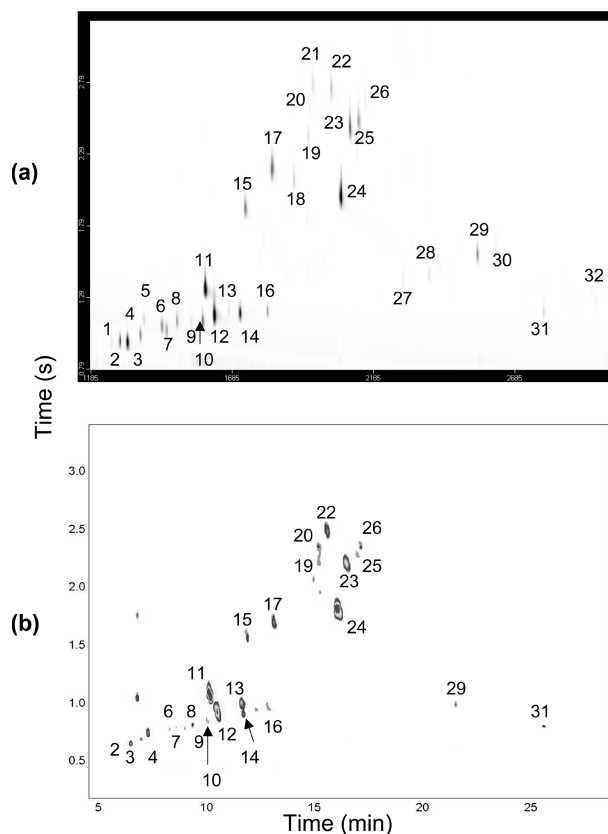


Figure 6. Analysis of a lemon thyme essential oil. Inset (a) is the chromatogram obtained from the LECO Pegasus 4D, GCxGC-TOFMS. Inset (b) is the chromatogram of the same essential oil analyzed on the low-resource breadboard GCxGC instrument. Initial temperatures of 30 and 80°C were used for the first column and second column, respectively. After 3 min of isothermal operation, both columns were ramped at 5°C/min to a temperature of 200 and 250°C, respectively. A modulation period of 4.0 s was used on both systems. A list of identified compounds based upon normalized retention time is found in Table 2.

tor cooling after a heating cycle. This protracted elevated temperature results in sample breakthrough. When the programmed voltage is used, peak streaking and sample loss through the hot modulator is substantially reduced. Clearly, from this qualitative study, using a variable voltage helps minimize sample loss for the highly volatile components.

Figure 6 is from a lemon thyme essential oil sample that was analyzed on a LECO Pegasus 4D GCxGC-TOFMS instrument (a) as well as the bench-top instrument described here (b). Both the Pegasus 4D instrument and the bench-top were operated under similar chromatographic conditions and used similar columns. Initial temperatures of 30 and 80°C were used for the first column and second column, respectively. After 3 min of isothermal operation, both columns were ramped at 5°C/min to a temperature of 200 and 250°C, respectively. The

Table 2. Thirty-two major compounds of a lemon thyme essential oil sample identified by a LECO Pegasus 4D, GCxGC-TOFMS. Data processing was performed by ChromaTOF software, and identified compounds are based upon the spectral match from the NIST library. Normalized retention times were used for comparison between the GCxGC-TOFMS and the bench-top GCxGC system

| Peak no. | Name |
|----------|---|
| 1 | Methylene chloride |
| 2 | * 1,4- <i>p</i> -Menthadiene |
| 3 | * Bicyclo[3.1.1]hept-2-ene, 2,6,6-trimethyl-, (<i>trans</i> -) |
| 4 | * Camphene |
| 5 | Benzene, butyl- |
| 6 | * 1-Methyl-4-isopropyl-1,4-cyclohexadiene |
| 7 | * α -Pinene |
| 8 | * Pinene |
| 9 | * β -Phellandrene |
| 10 | * 2-Carene |
| 11 | * <i>o</i> -Cymene |
| 12 | * Eucalyptol |
| 13 | * 1,3,7-Octatriene, 3,7-dimethyl- |
| 14 | * 1,4-Cyclohexadiene, 1-methyl-4-(1-methyl-ethyl)- |
| 15 | * 4-Carene |
| 16 | * Terpinolen |
| 17 | * Linalyl alcohol |
| 18 | * Neryl alcohol |
| 19 | * Geranyl Alcohol |
| 20 | * L-Pinocarveol |
| 21 | * Carveol |
| 22 | * L-Borneol |
| 23 | * 3-Carene |
| 24 | * Terpenol |
| 25 | * (E)-3-Carene-2-ol |
| 26 | * <i>cis</i> -Piperitol |
| 27 | * 2,6-Dimethyl-1,5,7-octatriene |
| 28 | * Acetic acid, 1,7,7-trimethyl-bicyclo[2.2.1]hept-2- |
| 29 | * α -Terpinyl acetate |
| 30 | * Neryl acetate |
| 31 | * Caryophyllene |
| 32 | * Gurjunene |

* denotes identified compound on bench-top system determined by normalized retention time.

temperature ramping of the second column on the Pegasus 4D system was set with an upper limit of 225°C because the first few centimeters of the second column (PEG) is used for modulation. The hot-jet gas temperature on the Pegasus 4D modulator was set 30°C above the second-column temperature and a hot-pulse time of 0.4 s was used. Temperature limitations for the second column (PEG) therefore limit the maximum temperature to 220°C. However, in spite of this temperature limitation, all compounds eluted prior to the second column reaching 220°C on both systems. A modulation period of 4.0 s was used on both systems.

The sample was diluted with methylene chloride 1:10 prior to injection on both systems. Peak identification on

the Pegasus 4D was performed with LECO ChromaTOF software and a list of the major compounds is displayed in Table 2. Peak characterization on the bench-top GC × GC system is based on retention time normalization and matching with the data acquired from the Pegasus 4D.

The two chromatograms are very similar, with the exception of two artifacts that are present on Fig. 6b above compound 2 (1,4-*p*-menthadiene). Over 1300 identified peaks with an S/N greater than 100 were detected with the Pegasus 4D and ChromaTOF software. Of these, 32 compounds were identified with an S/N greater than 100 and a spectral similarity greater than 800 out of a possible 1000. The spectral similarity is defined as the degree of similarity of the acquired mass-spectra as compared with a similar mass-spectra match found in the instrument library. A complete list of the 32 compounds identified by the LECO software is displayed in Table 2. Of the 32 major compounds identified by the ChromaTOF software, 24 matched with the normalized retention times on the GC × GC-FID bench-top system.

4 Concluding remarks

This bench-top system is a first step in the development of a field-portable GC × GC instrument. The use of at-column heating has eliminated the need for a convection oven and decreased the footprint and weight of the GC × GC. A resistively heated and closed-loop liquid-cooled thermal modulator remedies the use of cryogenic materials needed for commercial thermal modulators. In addition, the use of liquid-cooling for the modulator increases trapping performance for volatile compounds with boiling points at or below hexane.

The most significant limitation of the single-stage, low-resource thermal modulator described here is the higher quiescent trapping temperature (−30°C) relative to temperatures that can be achieved by cooling with cryogenic materials. However, the use of a programmable applied voltage for modulator heating decreases sample loss associated with single-stage modulators.

Streaking on the GC × GC chromatograms has been reduced, suggesting that the modulator is returning to a trapping temperature faster than when using air as a cooling medium. Continued work in the area of miniaturization the liquid-cooling pump, liquid chiller, power supply, and modulator housing are under investigation.

The authors would like to thank the Jet Propulsion Laboratory (JPL), Director's Discretionary Funding for financial support; Bruce Block, Department of Atmospheric, Oceanic and Space Science, the University of Michigan for technical discussions and shop services; Sunghuyn Lee, Department of Mechanical Engineering, the University of Michigan for his contribution to the modula-

tor heating; RVM Scientific, Santa Barbara, CA for the LTM columns; LECO Corporation, St. Joseph, MI, for the Pegasus 4D GC × GC-TOFMS instrument; Dr. Megan McGuigan, University of Michigan, for sample analysis on the LECO instrument; and P. T. Stevens, University of Michigan, for instrument design support.

5 References

- [1] Van Deursen, M., Beens, J., Reijenga, J., Lipman, P., Cramers, C., *J. High Resol. Chromatogr.* 2000, 23, 507–510.
- [2] Ledford, E. B., Billesbach, C. A., *J. High Resol. Chromatogr.* 2000, 23, 205–207.
- [3] Beens, J., Blomberg, J., Schoenmakers, P. J., *J. High Resol. Chromatogr.* 2000, 23, 182–188.
- [4] Seeley, J. V., Kramp, F. J., Sharpe, K. S., Seeley, S. K., *J. Sep. Sci.* 2002, 25, 53–59.
- [5] Schoenmakers, P. J., Oomen, J. L. M. M., Blomberg, J., Genuit, W., van Velzen, G., *J. Chromatogr. A* 2000, 892, 29–46.
- [6] Frysinger, G. S., Gaines, R. B., *J. High Resol. Chromatogr.* 2000, 23, 197–201.
- [7] Phillips, J. B., Beens, J., *J. Chromatogr.* 1999, 856, 331–347.
- [8] Dalluge, J., van Stee, L. L. P., Xu, X., Williams, J., *et al.*, *J. Chromatogr. A* 2002, 974, 169–184.
- [9] Liu, Z., Sirimanne, S. R., Patterson, D. G., Needhan, L. L., Phillips, J. B., *Anal. Chem.* 1994, 66, 3086–3092.
- [10] Dimandja, J. M., Stanfill, S. B., Grainger, J., Patterson, D. G., *J. High Resolut. Chromatogr.* 2000, 23, 208–214.
- [11] Marriott, P. J., Shellie, R., Fergeus, J., Ong, R., Morrison, P., *Flavour Frag. J.* 2000, 15, 225–239.
- [12] Lewis, A. C., Carslaw, N., Marriott, P. J., Kinghorn, R. M., *et al.*, *Nature* 2000, 405, 778–781.
- [13] Venkatramani, C. J., Xu, J., Phillips, J. B., *Anal. Chem.* 1996, 68, 1486–1492.
- [14] Marriott, P. J., Kinghorn, R. M., *Anal. Sciences* 1998, 14, 651–659.
- [15] Beens, J., Adahchour, M., Vreuls, R. J. J., van Altena, K., Brinkman, U. A. Th., *J. Chromatogr. A* 2001, 919, 127–132.
- [16] Marriott, P. J., Kinghorn, R. M., *Anal. Chem.* 1997, 69, 2582–2588.
- [17] Ledford, E. B., Billesbach, C., *J. High Resol. Chromatogr.* 2000, 23, 202–204.
- [18] Pursch, M., Sun, K., Winniford, B., Cortes, H., *et al.*, *Anal. Bioanal. Chem.* 2002, 373, 356–367.
- [19] Libardoni, M., Waite, J. H., Sacks, R., *Anal. Chem.* 2005, 77, 2786–2794.
- [20] Mustacich, R., Everson, J., Richards, J., *Am. Laboratory* 2003, 3, 38–41.
- [21] Whiting, J., Sacks, R., *Anal. Chem.* 2003, 75, 2215–2223.
- [22] Leinhard, J. H. IV, Leinhard, J. H. V., *A Heat Transfer Textbook*, 3rd Edn., Phlogiston Press, Cambridge, MA 2005, pp. 341–385.
- [23] Holman, J. P., *Heat Transfer*, McGraw-Hill – Education, Berkshire, UK 2001.
- [24] Churchill, S. W., Bernstein, M., *J. Heat Trans. ASME, Ser. C.* 1977, 99, 300–306.